

## The AMS-02 experiment on the ISS

This article has been downloaded from IOPscience. Please scroll down to see the full text article.

2009 J. Phys.: Conf. Ser. 171 012045

(<http://iopscience.iop.org/1742-6596/171/1/012045>)

View [the table of contents for this issue](#), or go to the [journal homepage](#) for more

Download details:

IP Address: 79.18.63.57

The article was downloaded on 11/09/2011 at 14:31

Please note that [terms and conditions apply](#).

# The AMS-02 experiment on the ISS

**Jorge Casaus**

Dpto. Investigación Básica, CIEMAT, Avda. Complutense 22, 28040 Madrid, Spain

E-mail: [jorge.casaus@ciemat.es](mailto:jorge.casaus@ciemat.es)

**Abstract.** The Alpha Magnetic Spectrometer (AMS-02) on the International Space Station (ISS) is a large acceptance magnetic spectrometer aiming for high precision studies of cosmic rays in space. The experiment will address fundamental questions regarding primary antimatter and dark matter contents of the universe. In addition, the precise measurements of cosmic rays in a wide energy range will result in a greatly improved understanding of the cosmic ray propagation in the Galaxy. The detector is now in its final assembly stage at CERN (Geneva) and it will be shipped to KSC (Florida) for integration with the space shuttle Discovery before the end of 2009. The STS-134 mission, currently scheduled for launch in September 2010 will transport the experiment to the ISS where it will operate for a period of 3 to 5 years.

## 1. Introduction

The asymmetry between matter and antimatter in the universe is one of the most important open questions in particle physics. The question whether there are cosmologically sizable antimatter domains in the universe has deep impact on the foundations of the theories of particle physics, namely, CP-violation and baryon number non-conservation. The apparent absence of antinuclei in cosmic rays together with the lack of anomalous  $\gamma$ -ray observations originating from annihilation products are usually taken as an evidence for the standard baryogenesis approach [1]. However, baryogenesis models imply baryon number non-conservation and large levels of CP-violation which are not yet supported by particle physics experimental data. Alternative solutions which allow the present existence of primordial antimatter have been developed [2] (see also the reviews [3,4]). The predictions of some of these theories, which could imply antimatter domains in the Galaxy [5], may be achievable with sensitive searches for antinuclei in cosmic rays.

Cosmological observations are consistent with the presence of dark matter (DM) as the major matter component of the universe [6]. Moreover, the observation of galactic rotation curves indicates [7] the presence of non-luminous haloes which dominate the gravitational evolution of galaxies. On the other hand, simulations of large scale structure or galactic formation [8] favor weakly interacting massive particles (WIMPs) as the main component needed to reproduce the observations. Among various proposed DM candidates [9], the neutralino [10], within the framework of supersymmetric extensions of the Standard Model, and the Kaluza-Klein particles [11], resulting from theories involving compactified extra dimensions, provide distinctive experimental signatures. The annihilation products of these candidates in the halo of the Galaxy could be detected as deviations in the fluxes of antiparticle species (positron, antiproton, antideuteron) and  $\gamma$ -rays [12].

In recent years, there has been growing experimental evidence of an anomalous excess in the positron fraction in the range 10–50 GeV [13–15] and in the electron plus positron flux in the 500–800 GeV region [16, 17] which can be interpreted either as the contribution of few nearby astrophysical sources (see e.g. [18]) or as an indication of DM annihilation in the galactic halo (see e.g. [19, 20]). Precise measurements in a wide energy range are required to confirm this signal and, eventually, reveal its nature. In particular, the absence of evidence of any deviation in the antiproton spectrum sets strong constraints on the properties of the DM candidates.

The expected fluxes of ordinary galactic cosmic rays is based on models which account for their origin and propagation in the Galaxy [21, 22]. The current program in cosmic ray propagation calculations aims to describe all primary and secondary species in galactic cosmic rays (hadrons and leptons) and diffuse  $\gamma$ -ray background within a single model. The free parameters in these models (composition and injection spectra and galactic disk and halo properties) can be derived from measurements done in the heliosphere. However, only precise knowledge of the elemental and isotopic spectra of hadronic cosmic rays in a wide energy range can validate the models and pin down the uncertainties on their free parameters.

The faint signal searches in cosmic rays are difficult on earth due to the Earth's atmosphere shielding. The inaccessibility to the primary impinging particle prevents a precise identification and measurement. A space flight provides the appropriate environment for precision measurements.

AMS [23] is a general-purpose experiment intended to perform measurements of charged cosmic rays with unprecedented statistics and sensitivity to faint signals. The large acceptance, long exposure and the detector identification capabilities in a wide energy range will improve by orders of magnitude the present knowledge of cosmic rays.

In this paper, a general description of the experimental program will be presented. The results obtained from a 10-day flight on the space shuttle of a prototype of the spectrometer will be summarized. The detector components and the expected performances for the long exposure run (3–5 years) on the ISS will be discussed in the last sections.

## 2. Experimental program

The AMS experiment is a fundamental physics experiment in space. The questions addressed by the experiment deal with the basics of our understanding of the universe. The AMS project is a joint effort between NASA and a collaboration of 50 High Energy Physics institutes from Europe, Asia and US and it involves more than 500 physicists and engineers.

The AMS experimental program is divided into two phases: a precursor flight on the space shuttle and a long exposure flight on the ISS.

The use of the space shuttle and the space station follows from an agreement between NASA and the US Department of Energy, signed in 1995, which states that the AMS collaboration has full responsibility on the detector design, operation and scientific objectives of the experiment. NASA provides the space transportation and installation and supervises all the safety critical issues.

After the completion of the first phase of the experiment, the tragic loss of the orbital vehicle Columbia in 2003 brought into peril the second phase of the AMS program. It is only very recently that an additional shuttle flight for AMS has been allocated [24]. The STS-134 mission to transport AMS to the ISS onboard the space shuttle Discovery is currently scheduled in September 2010 [25].

## 3. The precursor flight

A prototype of the AMS detector, AMS-01, was flown on the space shuttle Discovery on 2–12 June 1998 (STS-91 mission). The main purpose of the precursor flight was to test the spectrometer design principles and to gain experience in the operation of the detector under real

conditions. In addition, the STS-91 orbital parameters, similar to those of the ISS, allowed to study the expected backgrounds for faint signal searches.

The success of the 10-day mission (about 200 hours of data taking with 100 million physical triggers) allowed to obtain relevant results concerning particle fluxes in near Earth orbit [26–30] and improved limits on the presence of primary antimatter [31,32]. In particular, the cosmic ray positron fraction, measured in the energy range of 1–30 GeV [14] as shown in Fig. 1, provided an independent confirmation of the excess above 10 GeV.

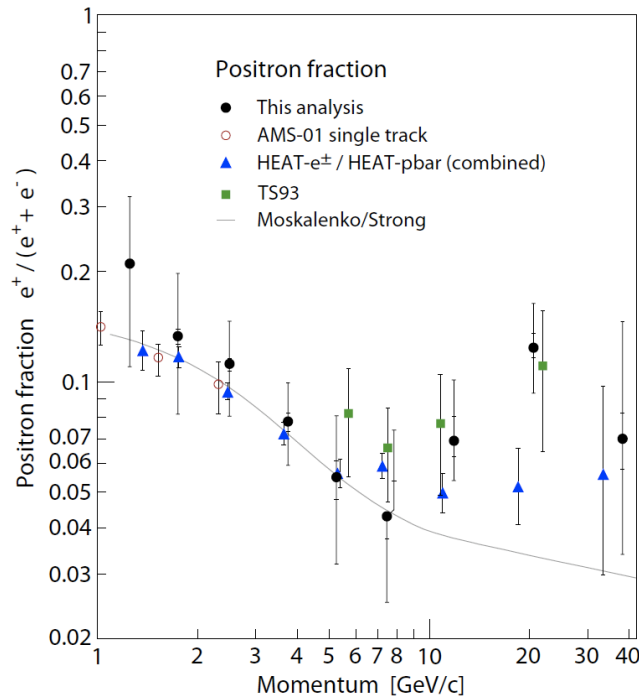


**Figure 1.** The positron fraction measured by AMS-01 using converted bremsstrahlung photons (reprint from [14]). The results (filled circles) are compared with earlier results from AMS-01 (open circles) [28], TS93 (squares) [33], the combined results from HEAT- $e^\pm$  and HEAT-pbar (triangles) [13], together with a model calculation for purely secondary positron production from [34] (solid line). The total error is given by the outer error bars, while the inner bars represent the systematic contribution to the total error.

In spite of the successful 10-day operation of the AMS-01 prototype, the 3–5 year operation on the ISS required a major redesign of the spectrometer to guarantee that the mission objectives could be reliably accomplished.

#### 4. Detector description

The AMS-02 detector is a large acceptance spaceborne magnetic spectrometer designed to perform precise measurements of charged cosmic rays in a wide energy range. The main components of the detector are displayed in Fig. 2. In AMS-02, the charged particle bending, provided by a superconducting magnet, is measured by a silicon tracker (STD). The particle time of flight, and hence its velocity, is determined by a set of scintillation counter hodoscopes (TOF). Additional particle identification capabilities are provided by a transition radiation detector (TRD), a ring imaging Čerenkov counter (RICH) and an electromagnetic calorimeter (ECAL). Finally, a shell of anticoincidence counters (ACC) covering the inner surface of the magnet provides a veto for non-fiducial particle trajectories.

In addition to the intrinsic constraints of a spaceborne detector, the design of the detector had to accomplish with strict weight and power budgets coming from shuttle transportation and ISS service limitations. The total weight of the detector is 6.8 t and the power consumption is 2 kW.

All subdetectors have undergone extensive space qualification tests to fulfill NASA safety regulations as well as to ensure the mission success. In addition, the performance of individual subdetectors have been validated in a series of in-beam tests.

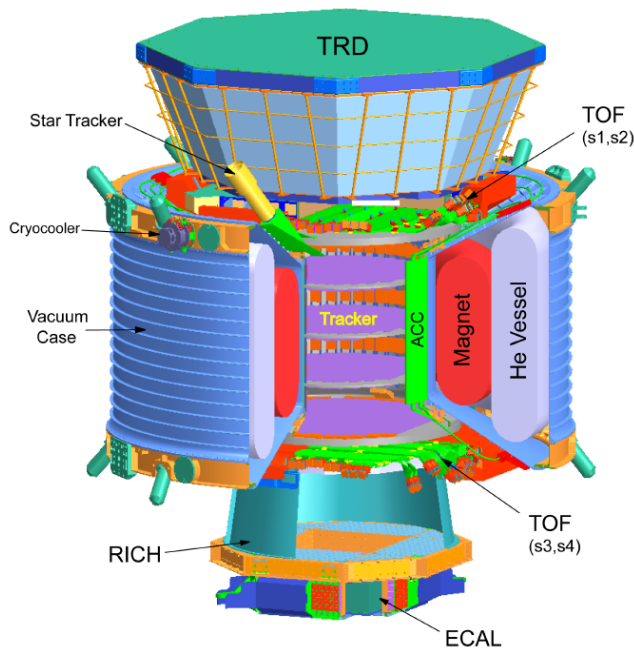


**Figure 2.** Schematic view of the AMS-02 spectrometer for the ISS. The superconducting magnet, the transition radiation detector (TRD), the time of flight (TOF), the silicon tracker, the ring imaging Čerenkov counter (RICH) and the electromagnetic calorimeter (ECAL) are shown. The external support structures, service electronics and thermal radiators surrounding the detector are not displayed.

The AMS-02 subsystems will be briefly described.

#### 4.1. Superconducting magnet

The cryogenic superconducting magnet [35] consists of an arrangement of 2 main dipole coils and 12 racetrack coils, a superfluid helium vessel and a cryogenic system, all enclosed in an aluminum vacuum tank which serves also as the primary structural support of the experiment. Supporting electronics, valves and cabling are located outside the vacuum tank. The vacuum tank itself has a toroidal shape with inner diameter 1.1 m, outer diameter 2.7 m and length of the central cylinder surrounding the STD 0.9 m. The geometry of the superconducting magnet defines the acceptance of the detector ( $0.5 \text{ m}^2\text{sr}$ ).

The magnet operates at a temperature of 1.8 K, cooled by means of the 2500 l of superfluid helium stored in the vessel. The higher latent heat and density of liquid  $^4\text{He}$  in its superfluid phase increases the total cooling capacity for a fixed helium tank volume. Moreover, the huge thermal conductivity of superfluid helium avoids significant temperature gradients. In zero gravity operation, this prevents temperature stratification which could result in unacceptable gradients across the magnet cold mass. Because of parasitic heat loads, the helium will gradually boil away throughout the lifetime of the experiment.

The dipole coils generate the magnetic field and the return coils control the stray field. The cryomagnet design ensures an intense and quite uniform field perpendicular to the vertical axis, a negligible dipole moment and the fulfillment of NASA safety regulations concerning fringe magnetic fields on the ISS.

The total weight of the system including the vacuum case is 2.4 tons and the nominal cryomagnet bending power is  $0.8 \text{ Tm}^2$ .

#### 4.2. Silicon tracker

The STD [36] consists of 8 layers of double-sided silicon micro-strip sensors which provide a position resolution of  $8.5 \mu\text{m}$  ( $30 \mu\text{m}$ ) in the bending (non-bending) plane. The total instrumented surface is  $6.45 \text{ m}^2$  with 196k readout channels.

The 8 layers are arranged in 5 thin support planes. The external ones are equipped with a single silicon layer whereas the central ones, located inside the magnet volume, mount one silicon layer on each side. The presence of the superconducting magnet requires an active cooling system to evacuate the heat generated by the STD front-end electronics. A laser system, which provides optically generated signals in the 8 STD layers, will monitor the system alignment throughout the mission.

The bending power provided by the magnet and the precise particle trajectory measurements in the STD provide a resolution in the rigidity measurement of 1.5% at 10 GV and a maximum detectable rigidity above 1 TV for protons. In addition, the wide dynamic range of the tracker readout electronics provides charge separation of nuclei up to  $Z=26$ .

#### *4.3. Time of flight*

The TOF system [37] consists of two double planes of scintillator counters located above the first and below the last tracker planes. Each plane consists of a set of 10mm thick scintillator paddles of different lengths and widths specially designed to match the magnet geometrical acceptance. The 34 paddles are connected on both ends to a total of 144 fine-mesh Hamamatsu R5946 photomultipliers through curved light guides which allow to align the photomultiplier axis with the magnetic fringe field to optimize its performance.

The time and position of the particle when traversing a paddle are derived from the high precision measurements at both sides of the each paddle. A resolution of 130 ps is obtained on the flight modules.

The TOF system provides the trigger to the experiment by coincidence. In addition, the precise time measurement allows a determination of the particle velocity with a resolution of 4%. Moreover, the measurement of the scintillation light produced in the counters provides a measurement of the particle absolute charge up to  $Z=20$ .

#### *4.4. Transition radiation detector*

The TRD [38] is composed of 20 layers of straw tube modules and polypropylene fiber radiators mounted in an octagonal structure. The upper 4 layers and the lower 4 layers are oriented in the perpendicular direction of the central 12 layers. The TRD is located on top of the experiment above the upper TOF plane and covers an area of  $2 \times 2 \text{ m}^2$ .

The 328 modules, built from 16 straw tubes each and operated at 1350 V with a mixture (80/20) of Xe and  $\text{CO}_2$ , are able to detect the transition radiation light produced by ultra relativistic particles on top of the energy loss by ionization in the gas. Moreover, the multiple measurements in the 20 layers of the detector provide additional information of the particle trajectory.

The TRD is able to perform electron to proton separation over the energy range 1.5–300 GeV with a rejection factor  $10^2$ – $10^3$  for 90% signal efficiency.

#### *4.5. Ring Imaging Čerenkov Counter*

The RICH [39] makes use of the proximity focusing technique and it is built of three main components. The Čerenkov radiator, attached to the lower TOF structure, is a mixture of 92 25mm-thick silica aerogel tiles with low refractive index ( $n=1.05$ ), covering 90% of the geometrical acceptance, and a central square with 16 5mm-thick sodium fluoride tiles. The detection plane, instrumented with 680 R7600-00-M16 multianode Hamamatsu photomultipliers for a total of 10880 readout channels, and the external conical reflector, which covers the 468 mm expansion length between the radiator and the detection plane.

The RICH measures the opening angle of the Čerenkov cone for relativistic particles and thus provides a precise particle velocity measurement ( $\sigma(\beta)/\beta < 0.1\%$ ). In addition, the account of

the light collected along the Čerenkov pattern provides a determination of the absolute charge for  $Z < 26$  with a  $10^{-2}$  charge confusion probability.

#### 4.6. Electromagnetic Calorimeter

The ECAL [40] consists of layers of lead foils with glued scintillating fibers. Every 11 layers are arranged into a superlayer with the fibers oriented along the same direction. The complete setup includes 9 superlayers with alternating fiber directions which results into a total radiation depth of  $16 X_0$  for shower development.

The scintillation light is transported by the fibers to a set of photomultiplier tubes located at the 4 sides of the central square active part. A total of 1296 readout channels (324 Hamamatsu R7600-00-M4 multianode PMTs) provide a 3D image of the electromagnetic shower with 18 samples in depth.

The electromagnetic calorimeter provides the experiment with a precise measurement of the energy of electromagnetic particles and an electron to proton separation in a wide energy range. The energy resolution is 3% for 100 GeV electrons and the achieved hadron rejection factor is  $10^4$  for  $E < 1$  TeV. In addition, thanks to the imaging capabilities of the detector, the shower shape reconstruction allows to determine the particle direction with an resolution better than  $1^\circ$  for  $E > 100$  GeV.

#### 4.7. Anticoincidence Counters

The ACC [41] consists of 16 scintillator panels arranged in a cylindrical shell around the STD. The scintillation light is driven by wave length sifting fibers and clear fibers to 16 Hamamatsu R5946 photomultiplier tubes.

The anticoincidence counters provide a trigger veto to particles entering the detector volume from the side. A highly efficient detection is needed to avoid contaminations in the antimatter searches and to reduce the trigger rate to acceptable levels. The ACC inefficiency has been measured to be below  $10^{-4}$ .

### 5. Expected performances

The AMS-02 detector design, the large geometrical acceptance ( $0.5 \text{ m}^2 \text{ sr}$ ) and the long exposure of the experiment will allow to extend the present range of precise measurements up to energies of  $O(1 \text{ TeV})$ .

The detector strategy is based on redundant measurements which ensure the required background rejection for rare signal searches. The electron hadron rejection makes use of both TRD and ECAL measurements to reach a rejection factor of  $10^6$  up to 300 GeV. The particle absolute charge measurement is based on tracker, TOF and RICH for light nuclei with an expected proton helium confusion probability below  $10^{-9}$ . In addition, the precise velocity measurements provided by the RICH allow to perform light isotope separation for  $E < 10$  GeV/n.

After a 3-year exposure, the experiment will collect  $10^9$  helium nuclei which will allow to discover (set a limit to) a relative flux of antihelium to helium at the  $10^{-9}$  level up to  $O(1 \text{ TeV})$ . Antiprotons will be identified up to 350 GeV with a total expected statistics of about  $10^6$  events. Concerning the primary hadron flux measurements, AMS-02 will collect  $10^8$  protons and  $10^7$  He with energies above 100 GeV/n and  $10^5(10^4)$  B(C) with  $E > 100$  GeV/n and it will precisely measure the individual element fluxes up to energies  $O(1 \text{ TeV/n})$ . As regards the light isotope separation, AMS-02 will identify  $10^8$  deuterium ( $^3\text{He}$ ) nuclei from protons ( $^4\text{He}$ ) up to 10 GeV/n. In addition, the ratio of the radioactive  $^{10}\text{Be}$  to the stable  $^9\text{Be}$  will be measured up to energies around 10 GeV/n. With respect to the lepton component, AMS-02 will measure the electron flux up to energies  $O(1 \text{ TeV})$  and it will identify and measure positrons up to 350 GeV.

Few examples of the fundamental physics studies which can be carried out with the data samples described above will be outlined.

According to a possible scenario with matter–antimatter domains within the Galaxy in a matter dominated universe [42], which is one of the experimentally non excluded matter–antimatter asymmetric models [43], antimatter coming from a globular-like star cluster could reach the heliosphere. The observed  $\gamma$ -ray spectrum sets an upper limit on the mass of the cluster of  $\sim 10^5$  solar masses. On the other hand, the globular cluster mass should exceed  $\sim 10^3$  solar masses to survive annihilation. Within this limits, an antihelium to helium flux ratio in cosmic rays ranging from  $10^{-6}$  to  $10^{-8}$  is expected. The AMS sensitivity is thus beyond the predicted limits for such a model.

Regarding the dark matter detection capabilities, AMS-02 provides a unique opportunity to perform a multichannel search for WIMP annihilation in the galactic halo. Recently released results, confirming the excess in the positron ratio at energies above 10 GeV and, independently, the structure in the electron and positron fluxes in the range from 500 to 800 GeV have been interpreted as signatures of DM annihilation. Models fitting this experimental signature are further constrained by the antiproton flux measurements, which are in agreement with the expectations from secondary production. The expectations for AMS-02 on the measurement of the positron ratio in the scenario of a Kaluza-Klein particle of 250 GeV/ $c^2$  fitting current measurements of the positron ratio is shown in Fig. 3. Alternatively, the measurements of electron and positron fluxes at higher energies can be fitted to a model with a Kaluza-Klein particle of 550 GeV/ $c^2$ . The expectations for AMS-02 on the measurement of the electron flux within this scenario is shown in Fig. 4. On the other hand, the precise measurement of the antiproton flux provided by AMS-02, shown in Fig. 5, will be highly sensitive to distortions generated by exotic contributions to the predicted secondary spectrum.

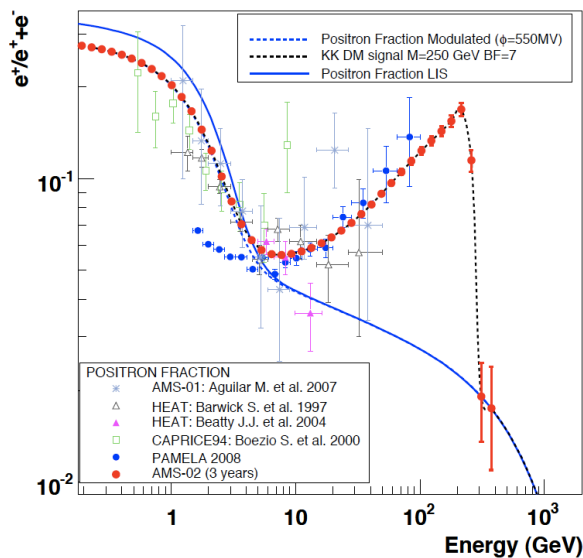


**Figure 3.** The AMS-02 positron fraction sensitivity to the signal from a model with a Kaluza-Klein particle with a mass of 250 GeV/ $c^2$  which fits the reported excess in the 10–50 GeV region [13–15] on top of a model calculation for purely secondary positron production from [34] (solid line).

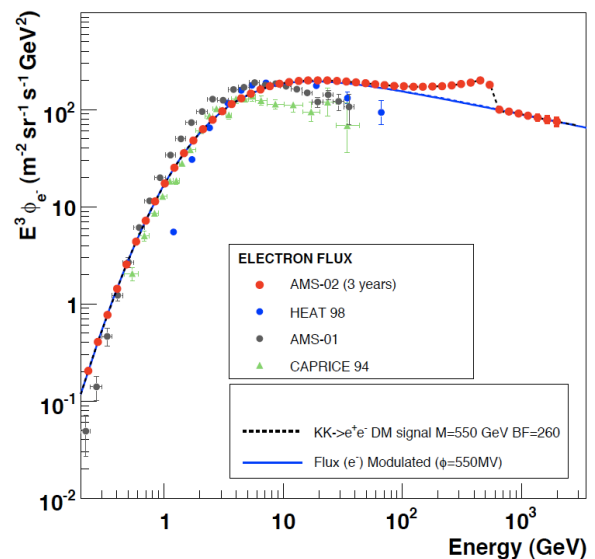


**Figure 4.** The AMS-02 electron flux sensitivity to the signal from a model with a Kaluza-Klein particle with a mass of 550 GeV/ $c^2$  which fits the reported excess in the 500–800 GeV region [16, 17] on top a of a model calculation from [34] (solid line). Recent measurements of the electron fluxes [28,44,45], scaled by  $E^3$ , are also shown.

The computation of the antimatter components in standard cosmic rays, and therefore the



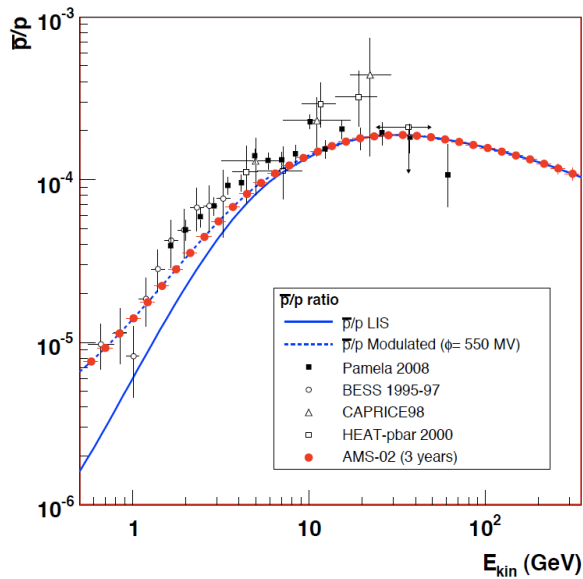


**Figure 5.** The AMS-02 expected sensitivity to the antiproton to proton ratio compared to recent measurements [46–49]. The expected ratio follows the propagation model described in [50].

background level for the dark matter search requires precise knowledge of the propagation parameters of charged cosmic rays in the Galaxy in a wide energy range. AMS-02 will constrain the models for production, acceleration and propagation of cosmic rays with the simultaneous measurement of the hadron and lepton components. For instance, carbon is expected to be of primary origin, i.e., present at the cosmic ray sources, whereas boron is believed to be a spallation product of the primary carbon in its path through the interstellar medium. The ratio B/C is thus used to estimate the amount of matter traversed by cosmic rays since their acceleration. In specific models, this ratio defines the cosmic ray escape path length distribution (leaky-box model) or the spatial diffusion coefficient (diffusion models). Furthermore, the ratio of the  $\beta$ -radioactive  $^{10}\text{Be}$  to the stable  $^9\text{Be}$  can be used to determine cosmic ray confinement time in the Galaxy and, in diffusion models, the effective thickness of the galactic halo.

The AMS-02 capabilities for the precise measurement of the B/C and  $^{10}\text{Be}/^9\text{Be}$  ratios are illustrated in Figs. 6 and 7, where the expectations for a reduced exposure are compared to the current measurements (see [51] and references therein). These are only two examples of the basic measurements needed to validate the current models of galactic cosmic ray propagation and to constrain their free parameters. The precise measurements provided by AMS experiment will define the benchmark data for those models.

## 6. Summary and outlook

AMS is a fundamental physics experiment performed in space. After the successful flight of a prototype version of the experiment in a short precursor flight, the final version of the detector will be installed on the ISS for a long duration mission.

The large data sample collected after the experiment long exposure will allow a sensitive search for antimatter and dark matter signatures in cosmic rays as well as astrophysics studies regarding cosmic ray production, acceleration and propagation in the Galaxy.

Currently, the AMS-02 final integration phase is taking place at CERN. Full detector calibration with beam at CERN-SPS will be performed later this year. Then, the detector will be shipped to ESA facilities at ESTEC for final thermal tests in vacuum and electromagnetic interference verification. Early in 2010, the detector will be transported to KSC facilities to complete the pre-flight operations. In September 2010, onboard the space shuttle Discovery in the STS-134 mission, AMS-02 will be transported to the ISS where it will operate for a period of 3 to 5 years.

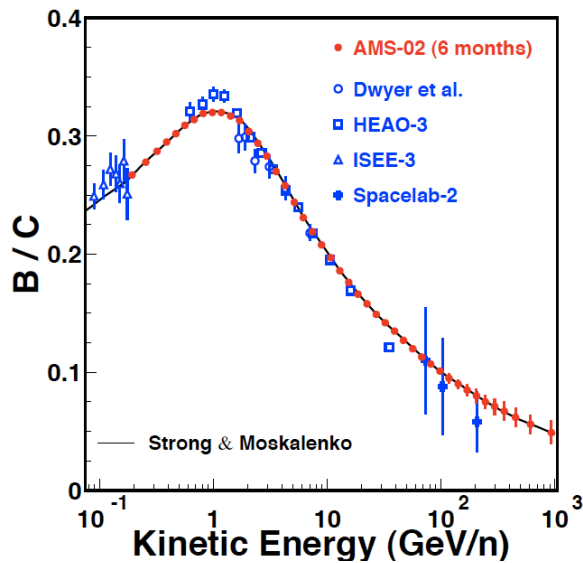


**Figure 6.** AMS-02 expected sensitivity on the B/C ratio after 6 months of data taking compared to present measurements [51]. The expected ratio follows the propagation model described in [21].

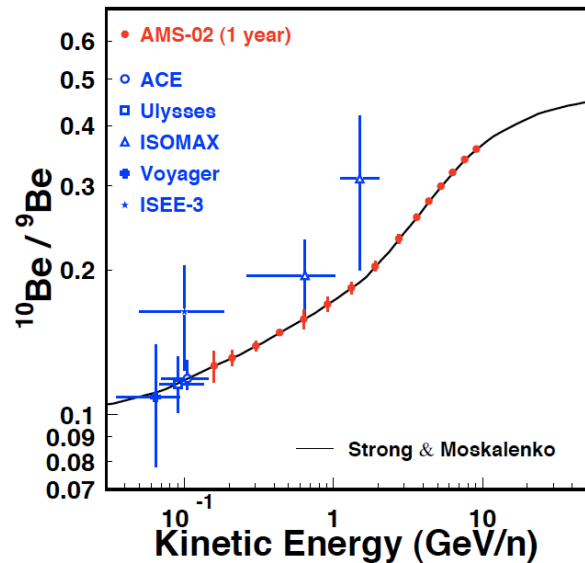


**Figure 7.** AMS-02 expected sensitivity on the  $^{10}\text{Be}/^9\text{Be}$  ratio after 1 year of data taking compared to present measurements [51]. The expected ratio follows the propagation model described in [21].

### Acknowledgments

I would like to thank D. Crespo and I. Cernuda for their help in the preparation of this document.

### References

- [1] S. Weinberg, *Phys. Rev. Lett.* **42** (1979) 850-853; E.W. Kolb, M.S. Turner, *Ann. Rev. Nucl. Part. Sci.* **33** (1983) 645-696
- [2] K.M. Belotsky, Yu.A. Golubkov, M.Yu. Khlopov, R.V. Konoplich, A.S. Sakharov, *Phys. Atom. Nucl.* **63** (2000) 233; Y.A. Golubkov, M.Y. Khlopov, *Phys. Atom. Nucl.* **64** (2001) 1821 (*Preprint astro-ph/0005419*); D. Fargion, M. Khlopov, *Astropart. Phys.* **19** (2003) 441 (*Preprint hep-ph/0109133*); A.D. Dolgov, M. Kawasaki, N. Kevlishvili, *Nucl. Phys. B* **807** (2009) 229 (*Preprint arXiv:0806.2986*)
- [3] Yu. Galaktionov, *Rep. Prog. Phys.* **65** (2002) 1243
- [4] D. Casadei, *Preprint astro-ph/0405417* (revised version in 2008)
- [5] C. Bambi, A.D. Dolgov, *Nucl. Phys. B* **784** (2007) 132 (*Preprint astro-ph/0702350*)
- [6] E. Komatsu *et al.*, *Preprint arXiv:0803.0547*; M. Kowalski *et al.*, *Ap. J.* **686** (2008) 749-778 (*Preprint arXiv:0804.4142*); W.J. Percival *et al.*, *Mon. Not. Roy. Astron. Soc.* **381** 1053-1066 (*Preprint arXiv:0705.3323*)
- [7] Y. Sofue, V. Rubin, *Ann. Rev. Astron. Astrophys.* **39** (2001) 137-174 (*Preprint astro-ph/0010594*)
- [8] V. Springel *et al.*, *Nature* **435** (2005) 629-636 (*Preprint astro-ph/0504097*)
- [9] G. Bertone, D. Hooper, J. Silk, *Phys. Rep.* **405** (2005) 279390 (*Preprint hep-ph/0404175*)
- [10] J.R. Ellis, J.S. Hagelin, D.V. Nanopoulos, K.A. Olive, M. Srednicki, *Nucl. Phys. B* **238** (1984) 453-476
- [11] G. Servant and T. M. Tait, *Nucl. Phys. B* **650** (2003) 391-419 (*Preprint hep-ph/0206071*)
- [12] N. Fornengo, *Adv.Space Res.* **41** (2008) 2010-2018 (*Preprint astro-ph/0612786*)
- [13] J.J. Beatty *et al.*, *Phys. Rev. Lett.* **93** (2004) 241102
- [14] M. Aguilar *et al.*, *Phys.Lett. B* **646** (2007) 145-154 (*Preprint astro-ph/0703154*)
- [15] O. Adriani *et al.*, *Preprint arXiv:0810.4995*
- [16] J. Chang *et al.*, *Nature* **456** (2008) 362-365
- [17] S. Torii *et al.*, *Preprint arXiv:0809.0760*
- [18] S. Profumo, *Preprint arXiv:0812.4457*
- [19] D. Hooper, A. Stebbins, K.M. Zurek, *Preprint arXiv:0812.3202*; D. Hooper, K.M. Zurek, *Preprint arXiv:0902.0593*

- [20] N. Arkani-Hamed, D.P. Finkbeiner, T. Slatyer, N. Weiner, *Phys. Rev. D* **79** (2009) 015014 (*Preprint arXiv:0810.0713*)
- [21] A.W. Strong, I.V. Moskalenko, *Ap. J.* **509** (1998) 212 (*Preprint astro-ph/9807150*)
- [22] D. Maurin, F. Donato, R. Taillet, P. Salati, *Ap.J.* **555** (2001) 585-596 (*Preprint astro-ph/0101231*)
- [23] S. Ahlen *et al.*, *Nucl. Instr. and Meth. A* **350** (1994) 351
- [24] *H.R.6063: National Aeronautics and Space Administration Authorization Act of 2008*, Public Law 110-422-OCT. 15, 2008
- [25] *NASA Flight Assignment Working Group (FAWG)*, Planning Manifest 23-Jan-2009
- [26] J. Alcaraz *et al.*, *Phys. Lett. B* **472** (2000) 215-226
- [27] J. Alcaraz *et al.*, *Phys. Lett. B* **490** (2000) 27-35
- [28] J. Alcaraz *et al.*, *Phys. Lett. B* **484** (2000) 10-22, Erratum-ibid. B **495** (2000) 440
- [29] J. Alcaraz *et al.*, *Phys. Lett. B* **494** (2000) 193-202
- [30] M. Aguilar *et al.*, *Phys. Rep.* **366** (2002) 331-405
- [31] J. Alcaraz *et al.*, *Phys. Lett. B* **461** (1999) 387-396
- [32] M. Cristinziani, *Nucl. Phys. Proc. Suppl.* **114** (2003) 275-279
- [33] R. L. Golden *et al.*, *Ap. J.* **457** (1996) L103
- [34] I.V. Moskalenko, A.W. Strong, *Ap. J.* **493** (1998) 694 (*Preprint astro-ph/9710124*)
- [35] B. Blau, *et al.*, *Nucl.Instr. and Meth. A* **518** (2004) 139-142; S.M. Harrison, *et al.*, *AIP Conf. Proc.* **823** (2006) 1315-1322
- [36] J. Alcaraz *et al.*, *Nucl.Instr. and Meth. A* **593** (2008) 376-398, Erratum-ibid. A **597** (2008) 270
- [37] L. Amati *et al.*, *Nucl. Phys. Proc. Suppl.* **150** (2006) 276-280
- [38] P. von Doetinchem *et al.*, *Nucl. Instr. and Meth. A* **558** (2006) 526-535 (*Preprint astro-ph/0608641*)
- [39] P. Aguayo *et al.*, *Nucl. Instr. and Meth. A* **560** (2006) 291-302
- [40] C. Adloff *et al.*, *Proc. 11th Int. Conf. Calorimetry in High-Energy Physics* (2004) 526-531
- [41] Ph. von Doetinchem, *et al.*, *Preprint arXiv:0811.4314*
- [42] M.Y. Khlopov, S.G. Rubin, d A.S. Sakharov, *Phys. Rev. D* **62** (2000) 083505 (*Preprint hep-ph/0003285*)
- [43] A.D. Dolgov, *Preprint arXiv:0806.4554*
- [44] M.A. DuVernois *et al.*, *Ap. J.* **559** (2001) 296-303
- [45] M. Boezio *et al.*, *Ap. J.* **532** (2000) 653-669
- [46] O. Adriani *et al.*, *Preprint arXiv:0810.4994*
- [47] S. Orito *et al.*, *Phys. Rev. Lett.* **84** (2000) 1078-1081 (*Preprint astro-ph/9906426*)
- [48] M. Boezio *et al.*, *Ap. J.* **561** (2001) 787-799
- [49] A.S. Beach *et al.*, *Phys.Rev.Lett.* **87** (2001) 271101 (*Preprint astro-ph/0111094*)
- [50] I.V Moskalenko, A.W. Strong, J.F. Ormes, M.S. Potgieter, *Ap. J.* **565** (2002) 280-296 (*Preprint astro-ph/0106567*)
- [51] J. Casaus, *Proc. 28th ICRC* **4** (2003) 2149